Available online at www.sciencedirect.com

jmr&t Journal of Materials Research and Technology

www.jmrt.com.br

Original Article

Fatigue behavior of PLA-wood composite manufactured by fused filament fabrication

J. Antonio Travieso-Rodriguez[a], *Mohammad D. Zandi*[a], *Ramón Jerez-Mesa*[b,*], *Jordi Lluma-Fuentes*[c]

[a] *Universitat Politècnica de Catalunya, Escola d'Enginyeria de Barcelona Est, Department of Mechanical Engineering, TECNOFAB Group. Av. d'Eduard Maristany, 10-14, 08019 Barcelona, Spain*

[b] *Universitat de Vic. Universitat Central de Catalunya, Faculty of Science and Technology, Department of Engineering, MECAMAT Group. C. de la Laura, 13. 08500 Vic, Spain*

[c] *Universitat Politècnica de Catalunya, Escola d'Enginyeria de Barcelona Est, Department of Science Materials and Engineering, PROCOMAME Group. Av. d'Eduard Maristany, 10-14, 08019 Barcelona, Spain*

ARTICLE INFO

Article history:
Received 16 March 2020
Accepted 1 June 2020
Available online 13 June 2020

Keywords:
PLA
Composite
Additive manufacturing
Fused filament fabrication
Endurance limit
Fatigue

ABSTRACT

In this paper, the fatigue behavior of a polylactic acid-based composite reinforced with wood (trademarked as Timberfill) processed through fused filament fabrication is analyzed through rotating bending fatigue tests. Originally, this material was developed with the aim of enhancing the resistance of PLA by increasing the inner friction between polymer filaments. This work aims to confirm whether the inclusion of wood delivers the expected mechanical advantages from a functional point of view. The effect of wood on the mechanical behavior of the material is also assessed by comparing the results to similar experimental observed on non-reinforced PLA specimens. Firstly, the optimal set of parameters and levels resulting in the highest number of cycles to failure are determined, and compared to those found for PLA, by applying a Taguchi L27 experimental array. Layer height, infill level and nozzle diameter prove to be the most influential parameters on fatigue life. During a second phase, a set of specimens manufactured through the best parameter set were tested at different stress levels to represent the S-N curve. Infinite life was observed for specimens loaded with a maximum stress of 17.9 MPa. Therefore, this value can be considered as a lower threshold of the endurance limit for Timberfill cylindrical parts subjected to cyclic bending stress. SEM observations reveal that wood has a detrimental effect on the PLA matrix, as is reduces the cohesion of deposited filaments, and increases the ductile behavior of the base material.

Abbreviations: AM, additive manufacturing; FDM, fused deposition modelling; FFF, fused filament fabrication; PLA, polylactic acid; ABS, acrylonitrile butadiene styrene; DOE, design of experiments; ANOVA, analysis of variance; SEM, scanning electron microscope.

* *Corresponding author.*
E-mail: ramon.jerez@uvic.cat (R. Jerez-Mesa).

https://doi.org/10.1016/j.jmrt.2020.06.003

1. Introduction

One of the most extended additive manufacturing (AM) technique is Fused Filament Fabrication (FFF), or Fused Deposition Modelling (FDM) as patented in 1991 by Stratasys. FFF machines generate a 3D object by extruding a filament of a heated material, which is accurately distributed onto successive layers driven by a numerical control routine, thus constructing the workpiece from the bottom to the top. [1] The fact that the process is driven my thermal dynamics and change of state of the material [2], coupled with the fact that the process is characterized by numerous parameters that have to be determined manually by users in open-source and small scale 3D printing devices, the mechanical properties of parts obtained by means FFF are uncertain [3].

This paper deals with a wood-reinforced PLA material, commercially named as Timberfill. This material was developed to offer consumers a way of generating wood-looking parts, while also expecting an increase of the inner friction between the extruded filaments to enhance its resistance. The interest around the addition of natural fibers as fillers for common materials for additive manufacturing has risen in the last years, mainly due to sustainability reasons. For instance, furniture waste can be recycled by adding it to these materials, thus extending its lifecycle [4], and the use of highly available materials such as bamboo, makes it a sustainable idea [5]. The increase of biodegradability of the material is also noticeable when natural fibers, such as kenaf fibers, are joint to the base material [6]. The advantages are not only sustaibilitywise, but also related to an eventual enhancement of mechanical properties. For instance, kenaf-reinforced PLA has proved to increase its strength up to 50% with regards to the pure material [7]. But however interesting this combination might be, other researchers have highlighted the need to confirm the positive effect of wood addition, as not all fibers have the same affinity with the base material, as highlighted Huber & Müssig (2008) by observing different cohesion capabilities of hemp, flax and cotton fibers that derived in irregular PLA reinforcement [8].

The effect of reinforcement is also not totally characterized if it is attempted by adding particles instead of longitudinal fibers. Tao et al. (2017) [9] observed that the interfacial adhesion between aspen sawdust and PLA was weak, what changed the thermal behavior of the composite, still adequate to be subjected to FFF. On the contrary, Kariz et al. (2018) [10] observed an increase of the tensile strength of wood-reinforced PLA from 55 MPa to 57 MPa with an addition of 10% wood, but a detrimental effect if that amount was higher, evidencing the high variability of results and the need to characterize specific materials for specific purposes. Lin et al. (2019) [11] also explored the ultraviolet aging as a means of improving the mechanical behavior of wood-reinforced PLA, finding that its effect is not positive at all. Ozdemir et al. (2014a) [12] proved that hot and cold water extraction of pine wood to later on reinforce a polypropylene matrix succeeded to improve the dimensional stability of parts manufactured with it. Therefore, as previous results go in different directions, it is necessary to understand the interaction between wood particles and PLA and assess its impact, whether positive or negative, as is done in this paper. The proliferous literature related to wood-reinforcement of PLA evidences the interest on the topic.

Most of research developed in this are has focused on tensile tests. Daver et al. (2016) [13] concluded that cork-reinforced PLA experienced an increase in ductility but lower mechanical properties as the percentage of cork increased, and that only a maximum of 5% of cork should be added to have a balanced effect. Gkartzou et al. (2017) [14] found that pine lignin dust is able to form heterogeneous systems with PLA, but again the adhesion can be detrimental. The effect of the reinforcement is also dependent of the length-to-diameter ratio of the particles. Depuydt et al. (2019) [15] conclude that short bamboo fibers increase twofold the elastic modulus of PLA, whereas the increase is more modest with dust-like fractions. Paulownia wood is also a feasible additive for PLA, and that it changes the tensile properties of the base material, as note by Tisserat et al. (2013) [16]. To a smaller extent, other mechanical properties of natural-fibers reinforcement of PLA have been tackled in bibliography. Guo et al. (2018) [17] deduced that a 10% addition of poplar wood could increase the impact strength of PLA by 7,75%. Flexural strength can also be increased by reinforcing PLA with thermomecanical pulp, with a higher chemical compatibility with PLA, as this enables better strength transfer from the material to the fibers [18]. A similar result was obtained by Ayrilmis et al. (2013) [19], proving that the bending and tensile strength of polypropylene was enhanced by reinforcing with walnut flour. In all cases, it seems that the extrusion temperature does not influence most of the physical properties of the material, at sight of the advances presented by Yang (2018) [20].

Other researchers have focused additional processing to make the reinforcement more effective, with diverse conclusions. Xie et al. (2017) [21] noted that the addition of plasticizers such as tributyl citrate can improve this adhesion and hence the mechanical properties and thermal stability of the composite. The positive effect of the addition of plasticizer was also supported by Stoof et al. (2017) [22] on hemp-reinforced PLA. Also, the crystallization rate of poplar-wood reinforced polypropylene could be enhanced by adding hexagonal boron nitride (Ayrilmis et al., 2014b) [23].

In contrast to the aforementioned references this paper does not aim to design a new material, but to assess the characteristics of one already existing and manufactured and distributed by a real company, by applying extensive experimental tests following a Taguchi orthogonal array. Furthermore, the study focuses on fatigue results, as this area of mechanical result has not been previously explored by other researchers on wood-PLA composite materials.

Focusing now on the FFF process itself, other authors have previously identified what are the most influential factors implicated that effectively define the mechanical behavior of workpieces. The revision presented henceforth has been used by the authors to decide which factors are to be analyzed in the experimental execution of this paper. For instance, it has been clearly observed that the manufacturing orientation determines the main stress carrying direction and should ideally coincide with the expected in-service loads of the part

to maximize its mechanical performance. Therefore, it is not worth considering it as a variable of study, but, on the contrary, as a fixed parameter [3,24,25].

All researchers agree that layer height is a very relevant parameter with impact on the mechanical properties of FFF parts, as it defines the neck growth that influences the cohesive forces between the deposited layers [26,27], especially when considering fatigue behavior. Tymrak et al. (2014) [27] concluded that by reducing the layer height to 0.2 mm, the tensile strength of PLA specimens was increased by 11.9 MPa, and the elastic modulus increased to 194 MPa. It also has a remarkable influence on the surface roughness and unitary cost of a piece, as show in their works Singh (2013a) [28] and Durgun & Ertan (2014) [29].

Another important aspect related to mechanical performance is how the infill is deposited to shape the overall geometry, defines the degree of porosity of the final part and the amount of bearing material [30]. Therefore, it accounts for the stiffness of the 3D printed part and its overall resistance [31]. How the infill is conformed actually depends on two different factors. On one hand, the infill density, that is, the space between filaments. And secondly, the infill pattern, as explains Wahl et al. (2012) [32].

Studies tackling with the fatigue performance of additive manufactured parts are scarce. Some references are found for laser sintered metal specimens in Spierings (2013) [33], Edwards & Ramulu (2014) [34] and Riemer et al. (2014) [35]. However, hardly have polymeric materials been previously explored. Afrose et al. (2016) [36], published a study dealing with the fatigue performance of PLA parts, where only one variable was considered, namely the manufacturing orientation. They found that specimens built at 45 degrees presented the highest fatigue life expected for every stress level tested. After that, Gomez-Gras et al. (2018) [3] used an experimental design to evaluate the fatigue performance of PLA. Both cases are an inspiration to this paper, especially the former, that is used as a reference point to evaluate the effects of the introduction of wood particles in the PLA matrix to generate the Timberfill composite.

The issue arising from using innovative commercial materials such as the PLA-wood composite considered in this paper is dually tackled in this paper. On one hand, the parameters recommended by the manufacturer have not been tested or confirmed experimentally, and therefore, should be confirmed experimentally. On the other hand, most authors publish recommendations for extended materials such as PLA, ABS, and non-commercial. For this reason, this paper has been developed to continuous working on the knowledge about printing parameters, focusing on fatigue behavior as response mechanism. As fatigue properties are not usually explored for additive manufactured parts especially wood-PLA composite, the novelty delivered by this paper is both composed by the special material it includes, and the response system studied. The results obtained and explained in this contribution are of high relevance for the industry and low scale manufacturing environments, as from it arise technological recommendations for the application of a composite material by means of open source devices, present nowadays in a high variety of economic sectors.

Table 1 – Reference mechanical properties and recommended manufacturing parameters specified by manufacturer for Timberfill material.

Property	Value	Property	Value
Material density	1.26 g/cm^3	Nozzle temperature	170–185 °C
Tensile strength*	39 MPa	Nozzle diameter	Min. 0.4 mm
Tensile modulus*	3200 MPa	Extruder velocity	20–30 mm/s

* Minimum guaranteed by the manufacturer.

Table 2 – Factors and levels used for the DOE.

Factor	Code	Level		
		1	2	3
Layer height [mm]	A	0.2	0.3	0.4
Nozzle diameter [mm]	B	0.7	0.5	0.6
Infill density [%]	C	25	50	75
Extrusion velocity [mm/s]	D	25	30	35

2. Materials and methods

The specimens used in this study were manufactured with Timberfill C̈hampagnëfilament with 2.85-mm diameter, developed and manufactured by Filamentum. Timberfill is a composite material, 100% biodegradable, consisting of a PLA matrix with an 8 ± 1% of wood fibers, as evidence thermogravimetric tests performed on the material. The tech specs provided by the manufacturer are included in Table 1. This material was developed with a purely aesthetic purpose, to imitate a wood appearance on objects, but also with the aim of enhancing resistance by increasing the inner friction between polymer filaments. This work aims to confirm whether the inclusion of wood delivers the expected mechanical advantages from a functional point of view.

2.1. *Taguchi experimental design*

Four main influential parameters on the fatigue performance of the Timberfill material were selected to perform the experimental design, namely the layer height, infill density, nozzle diameter and extrusion velocity. Three different experimental levels are considered to evaluate their influence on the fatigue lifespan response. The experimental execution was designed through a Taguchi orthogonal array. Each of the three levels selected for each factor are included in Table 2. This partial DOE method allows to combine numerous factors and levels and reduce the number of experiments.

Provided the number of factors and levels to be analyzed, the L27 array proves to be the most convenient to assess the first order influence of all factors, along with the mutual interactions among the first three ones [37]. Table 3 shows all the experimental runs described in the array. Each of them indicates the parameter set to be applied for all specimens manufacturing. Five specimens were manufactured to repeat each manufacturing condition. The selection of these factors was decided based on previous results observed by the group and published before.

Table 3 – L27 Taguchi orthogonal array for the DOE.

#run	Layer height [mm]	Nozzle diameter [mm]	Infill density [%]	Extrusion velocity [mm/s]
1	0.2	0.7	25	25
2	0.2	0.7	50	30
3	0.2	0.7	75	35
4	0.2	0.5	25	35
5	0.2	0.5	50	30
6	0.2	0.5	75	25
7	0.2	0.6	25	35
8	0.2	0.6	50	25
9	0.2	0.6	75	30
10	0.3	0.7	25	30
11	0.3	0.7	50	35
12	0.3	0.7	75	25
13	0.3	0.5	25	35
14	0.3	0.5	50	25
15	0.3	0.5	75	30
16	0.3	0.6	25	25
17	0.3	0.6	50	30
18	0.3	0.6	75	35
19	0.4	0.7	25	35
20	0.4	0.7	50	25
21	0.4	0.7	75	30
22	0.4	0.5	25	25
23	0.4	0.5	50	30
24	0.4	0.5	75	35
25	0.4	0.6	25	30
26	0.4	0.6	50	35
27	0.4	0.6	75	25

The effect of two infill patterns (rectilinear and honeycomb) was also included as a focus of study (Fig. 1), however excluded from the experimental array that experimental design repeated twice, once for each pattern. Consequently, 270 specimens were manufactured (5 specimens for 27 conditions). Samples with the same conditions have been printed to confirm the repeatability of the obtained results and provide the results of statistical significance.

2.2. *Specimens manufacture*

All the specimens have been manufactured using a PYRAMID 3D Studio RepRap 3D printer. The specimen geometry was reproduced according to the ASTM D7774 standard [38] that describes the method to test the flexural fatigue properties of plastics (Fig. 2). This standard was taken as a reference because there is no specific reference material to evaluate laminated or additive-manufactured polymer materials.

The printing parameters that are not object of study such as building orientation, raster angle, temperature, etc., were kept constant during the manufacturing process (Table 4). At the bottom layers, the volume was supported with a rectilinear gridded structure that was removed before the fatigue testing. Also, the specimens were manufactured with external perimeters, solid layers at the top and the bottom of two layers.

2.3. *Experimental setup*

A GUNTWP140 rotating bending stress machine has been used for the experiments (Fig. 3). The specimens were fixed to the chuck of the machine and rotated at a speed of 2800 min^{-1}. The inverted stress was applied by applying a load at its tip. The load was monitored during each test by a load cell installed at the loading mechanism. When the specimen fracture overcomes, the machine stops due to sensor displacement, and the number of cycles that each specimen endured is registered by a digital revolutions counter. The experimental setup was completed by a PCE-TC 3 thermographic camera

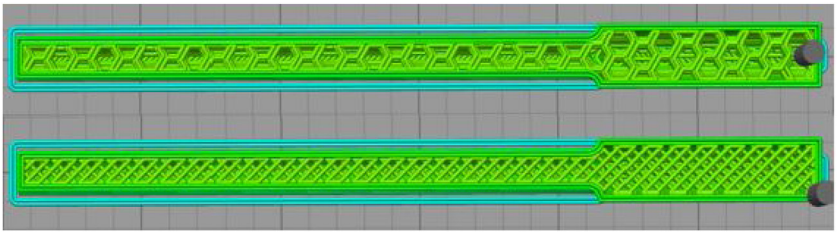

Fig. 1 – Top. Honeycomb infill pattern. Bottom. Rectilinear infill pattern. Blue lines: support material. Green lines: constitutive material of the specimen.

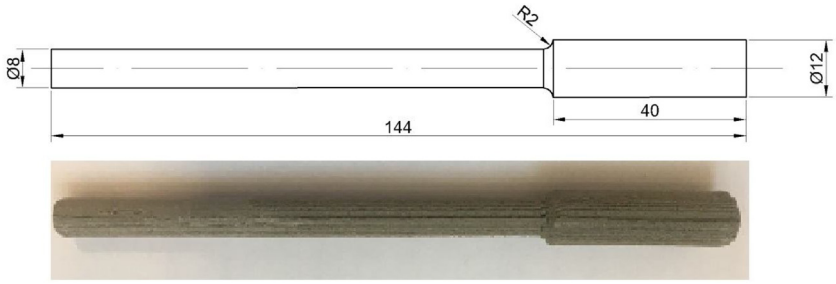

Fig. 2 – Top. Actual dimensions and shape. Bottom. Overview of the specimen manufactured.

Table 4 – Printing parameters kept constant during the experiments.

Orientation	Raster angle	Nozzle temperature	Skirt layer	Bed temperature
0○-X	45°	180 °C	2 layers	50 °C

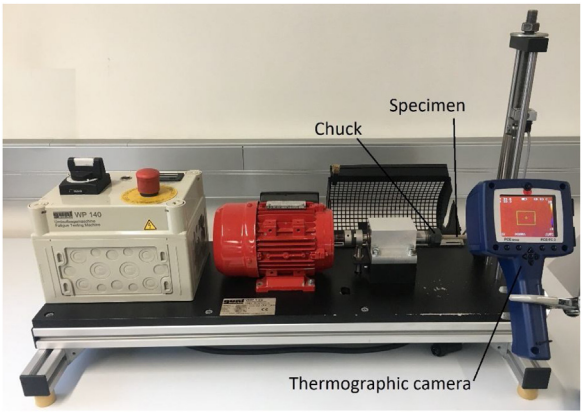

Fig. 3 – Overview of experimental setup.

with sensitivity of 32° C and precision of ±2° C to register the temperature of the specimen at its breaking point.

3. Results and discussion

In the first experimental phase, a single 10-N force is applied to all specimens, in order to identify the parameter set that leads to longer lifespan. Fig. 4 shows the results of the average number of cycles for each run, along with its standard deviation. The parameter combination leading to maximum fatigue life was found for run number 21, in both infill patterns. That means that the recommended manufacturing parameters should be 0.4-mm layer height, 0.7-mm nozzle diameter, 75% infill density and 35-mm/s printing velocity

As for the observed temperature recorded the fracture point in a range of 28.5–32.5 °C and no correlation was found between temperature and manufacturing conditions, it can be assumed that fatigue failure is not determined by yield of extreme temperature change.

3.1. *Analysis of variance*

The tested Taguchi arrays, for each infill pattern, were subjected to an analysis of variance (ANOVA) focusing on fatigue lifespan as response variable. To validate the statistical significance of the parameters included in the model, the p-value associated to each parameter included in the ANOVA was compared to a significance level of 5%. An Anderson Darling test was conducted to confirm the residual normality hypothesis of both sets of values was performed, to validate the ANOVA results, leading to a positive result.

Fig. 5 shows the influence of the manufacturing factors used on the specimens' fatigue life, including the aforementioned p-values. It can be concluded that the statistically significant factors are layer height, the nozzle diameter, and the density. Furthermore, the honeycomb infill reveals a higher mean result for the expected lifespan, meaning that it should be preferred to the rectilinear infill. This result has already been observed in other materials such as PLA [3] and ABS) [26].

The layer height has the highest effect on the life of the samples. In addition, it can be seen that higher layer heights derive in longer life of the specimens. Compared to other factors, the slope that defines this feature is higher, meaning that the response variable is much more sensitive to this parameter.

In terms of nozzle diameter, it appears that the best value is 0.7 mm, as it gives a longer life. This result explains that a higher nozzle diameter allows to deposit more material in one pass and increases the contact between filaments of different layers and the penetration of neck growth. This statement is only true because the range of layer heights included in the study range from 0.2 to 0.4 mm. Experience dictates that increasing the layer height to a value near to the nozzle diameter would have a detrimental effect, as the porosity of the part world increase.

The infill density has direct influence on fatigue lifespan, and should be maximized to have a positive effect, as it was expected. Finally, the manufacturing velocity has a high p-value. For this reason, it can be concluded that this factor does not have significant effect on the specimens' fatigue life. This could be caused because the velocities range studied is not wide enough. This fact is not important because open source FFF machines, do not allow the user to modify these values to a higher extent.

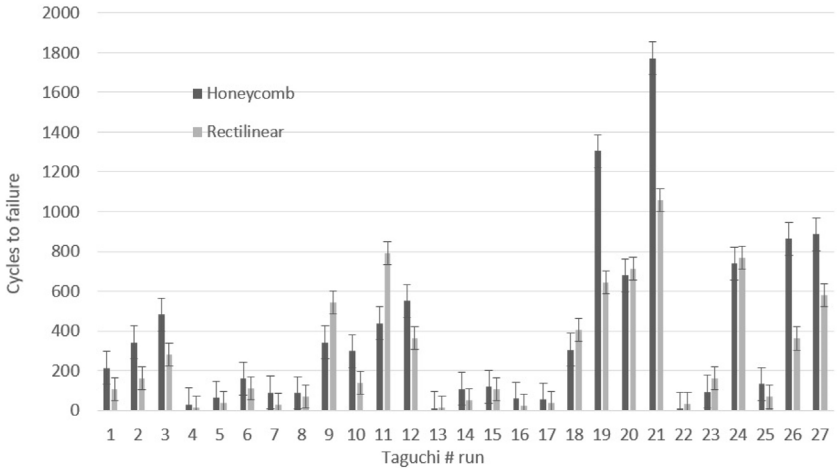

Fig. 4 – Average number of cycles to failure of each run.

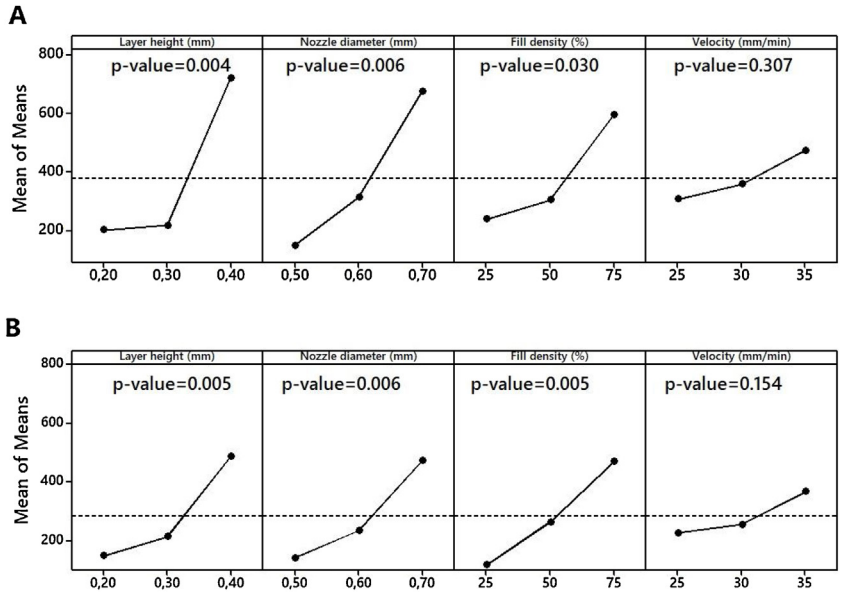

Fig. 5 – Main effects plot for the response variable number of cycles to failure and p-value associated to the ANOVA tests. (A) Honeycomb infill. (B) Rectilinear infill.

Table 5 – P-values for parameter interaction.

	Parameters interaction	p-Value
Honeycomb infill pattern	Layer height - Nozzle diameter	0.167
	Layer height - Fill density	0.355
	Nozzle diameter - Fill density	0.697
Rectilinear infill pattern	Layer height - Nozzle diameter	0.147
	Layer height - Fill density	0.212
	Nozzle diameter - Fill density	0.366

Interactions between the layer height, the nozzle diameter and the infill density were also assessed through the ANOVA analysis. The p-values obtained from the ANOVA analysis, included in Table 5, prove that no interaction is statistically significant between factors. Therefore, it is useless to draw conclusions of the interactions between parameters.

3.2. *Fractography*

Fractographies can deliver more information about the failure mode of the Timberfill material. The cross-sectional view of broken samples of the rectilinear (Fig. 6A) and honeycomb (Fig. 6B) at a 75% infill were taken by a Moticam 3 digital camera through a Motic SMC binocular. Both infills show ductile

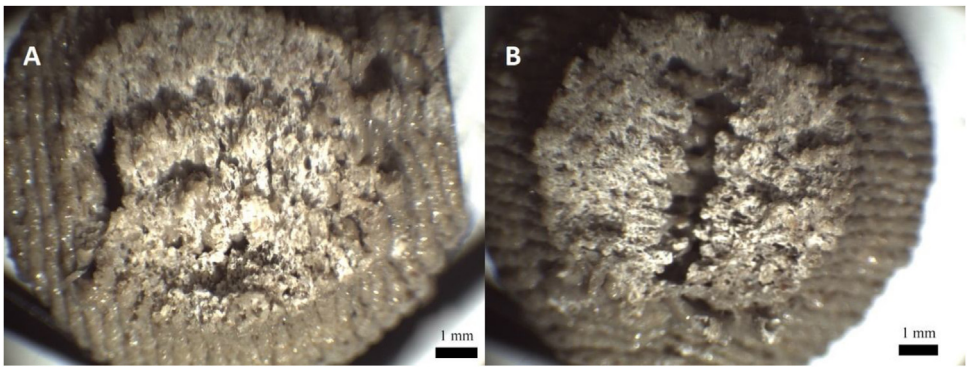

Fig. 6 – Fractographies of Timberfill specimens printed at 75% with infill pattern. (A) Rectilinear. (B) Honeycomb.

Table 6 – Optimal combination of factors and levels to maximize the expected cycles to failure.

Parameter	Values
Infill pattern	Honeycomb
Fill density	75%
Nozzle diameter	0.7 mm
Layer height	0.4 mm

Table 7 – Forces applied for the Wöhler curve tests and maximum stress levels.

F (N)	M_{max} (N·mm)	σ_{max} (MPa)
5.0	520	17.9
5.5	572	19.7
6	624	21.5
8.5	884	30.5
10.0	1040	35.8
11.5	1196	41.2
13.0	1352	46.6

behavior, with the presence of cavities and wooden particles separated by clearly distorted PLA walls. The distortion of the fracture surface is so remarkable that the deposited filaments can hardly be recognizable. Only the first and last printed layers show a less ductile pattern. This might be due to the fact that crack nucleation is originated at these zones.

3.3. *Wöhler curve for optimal printing conditions*

The results described at Section 3.1, evidence that there is a parameter set (Table 6) leading to higher fatigue lifespans. This parameter set was selected to manufacture a second set of specimens, in order to test them applying different stress levels to build the complete S-N curve, as indicates Table 7. As the FFF process improves the axial strength of the material due to the molecular alignment of the polymer chains, the two highest tested stresses are slightly higher than the minimum tensile strength guaranteed by the manufacturer.

Following the protocol established by Wirshing et al. (1980) [39], four repetitions were performed for each stress level, except for 35.8 MPa, which had been previously tested during the DOE phase. According to Burhan et al. (2018) [40], Palmgren's model in Eq. (1) represents the S-N curve for a composite material with an endurance limit.

Table 8 – Maximum stress levels included in the S-N curve of PLA specimens [4].

F (N)	M_{max} (N·mm)	σ_{max} (MPa)
10	1040	35.8
13	1352	46.6
15	1560	53.8
18	1872	64.5
20	2080	71.7
22	2288	78.8

$$S_a = S_f \left(2N_f\right)^b + S_\infty \quad (1)$$

where N_f are the cycles to failure, S_f is a constant typical of each type of specimen, S_a is the maximum stress to which they are subjected during the fatigue test, and S_∞ is the endurance limit.

The point cloud obtained from the previous testing was adjusted to a potential curve described by Eq. (1), obtaining a correlation with a Pearson's coefficient of 0.950. According to the executed tests, the specimens subjected to a maximum stress of 17.9 MPa did not experience failure before 10^6 cycles, hence this value being a lower threshold of the endurance limit of PLA-wood composite manufactured through FFF.

3.4. *Comparison between behavior of Timberfill and PLA*

Since the Timberfill material is a composite based on a PLA matrix, it is of interest to compare the results included in this paper with their analogous ones regarding non-reinforced PLA [3]. It is important to mention that the machine used to manufacture the specimens and the test procedure followed in both works are the same. In addition, the printer used was the same, which makes this comparison significant. However, the stress tested in these two materials were different, due to the fact that both materials present different yield points. Table 8 shows the maximum stress levels applied to PLA specimens.

The direct comparison of results show that the influence of each parameter on the fatigue life response shows the same behavior for both materials. The printing velocity shows no

influence, where layer height, nozzle diameter and infill percentage all have a direct relation to fatigue lifespan increase. That means that the PLA base in the composite material governs the general behavior of its derived composite, regardless of the wooden filling.

However, Timberfill seems more sensitive to the variation of the layer height, being this one the most relevant factor. On the other hand, the fatigue life for PLA specimens proved to be more influenced by the infill density. This difference could be explained by the fact that the wooden filling reduces the mobility between the polymer molecules, thus making the global infill density less relevant to achieve cohesion between all fibers. Meaning that, by having a PLA-wood composite, selecting the proper layer height has a higher influence to achieve the adequate resistance. In any case, the most important conclusion here is the similar influence of all parameters on the response.

Focusing now on the S-N curve, it can be observed that the exponent values differs about a 40% between both materials, being the expected life of Timberfill specimens lower than the one for non-reinforced PLA (Fig. 8). It is surprising that the introduction of wood as an additive in the PLA base is not positive, as one would expect that wood should improve resistance by acting as an anchoring point that limits polymer chain mobility. Instead, the wood seems to have the opposite effect: it does not act as a barrier for fracture prevention; much on the contrary, it weakens the PLA matrix.

This observation is confirmed through SEM inspection through JSM-7001 F mode of JEOL machine, which shows that the adhesion between the wood and the PLA fibers is detrimental, and the voids among fibers are more conspicuous than what PLA shows (Fig. 9). These discontinuities act as stress risers inside the volume and reduce the mechanical properties of the base material. For this reason, the crack leading to failure in the pure PLA polymer specimens does not spread as fast as in the Timberfill material. Therefore, the utilization of Timberfill should be limited to workpieces where aspect is more important than function.

The comparison between the failure mode of the Timberfill (Fig. 7) and PLA (Fig. 10) is also very revealing about the effect of wood introduction in the material. Whereas the non-reinforced PLA reveals a brittle behavior, the incorporation of wood inside the matrix induces a ductile failure mode of the walls between them. This change in the fracture mode could

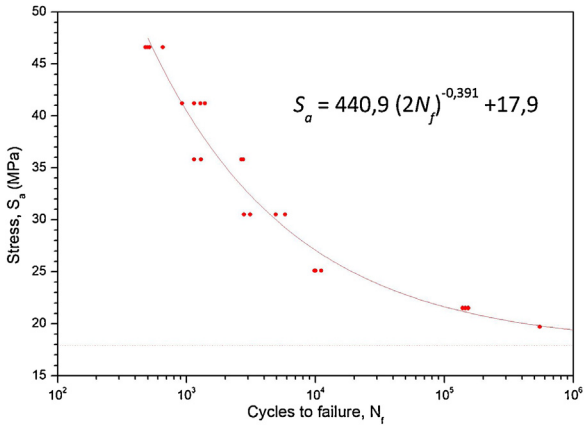

Fig. 7 – Wöhler curve for specimens manufactured with honeycomb infill, 0.4 mm layer height, 0.7 mm nozzle diameter, and 75% infill density.

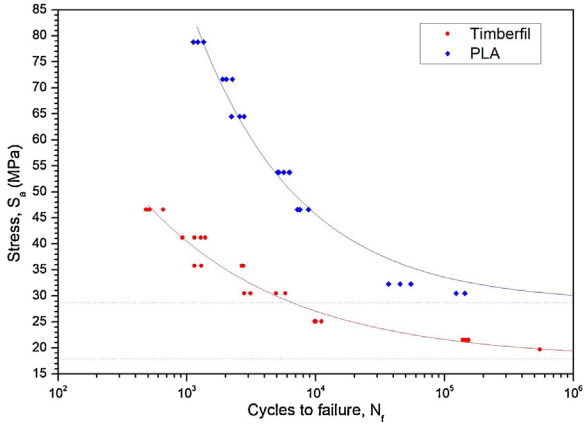

Fig. 8 – Wöhler curves for Timberfill and PLA.

be caused by the random distribution of voids and wood fibers that act as random oriented stress risers that change the local direction of the load inside the PLA matrix and prevents its failure by planes perpendicular to the nominal stress. Consequently, the matrix must tear between fibers and causes a much more ductile behavior.

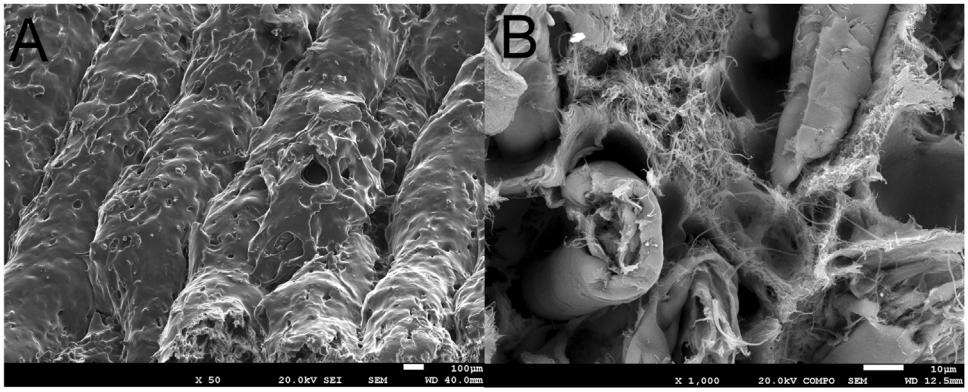

Fig. 9 – SEM images of Timberfil pieces. (A) Lateral view. (B) Detail of fractography.

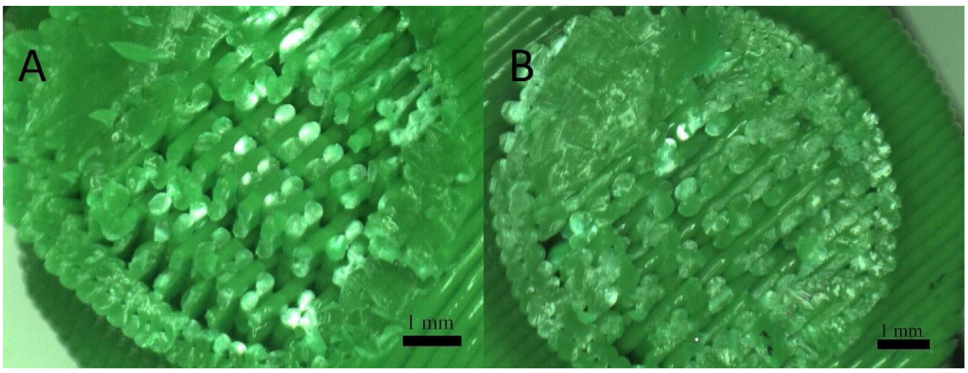

Fig. 10 – Fractographies of PLA specimens printed at the same conditions of Timberfill pieces with infill pattern. (A) Rectilinear. (B) Honeycomb.

4. Conclusions

A combination of three analysis, namely ANOVA performed on a Taguchi experimental design, the construction of an S-N curve, and microscopically observations was developed and explained in this paper to assess the mechanical behavior of a PLA-wood composite in terms of fatigue life. Only three parameters (nozzle diameter, layer height and infill density) out of four proved to be influential on the fatigue lifespan of cylindrical specimens subjected to rotating bending fatigue. The following conclusions can be extracted:

1 Specimens manufactured through a honeycomb pattern should be preferred to rectilinear ones to enhance fatigue life of PLA-wood parts. Furthermore, a combination of 75% infill density, 0.7 mm nozzle diameter and 0.4 mm layer height are recommended to manufacture this kind of work-pieces.
2 The printing velocity does not show influence on the results.
3 A lower threshold for the endurance limit was found at 17.9 MPa, for Timberfill manufactured with a parameter set described in the first conclusion.
4 The introduction of wood fibers has a detrimental effect on the PLA matrix in terms of mechanical behavior, as they reduce the adhesion between fibers, and increase the voids among them. These voids act as stress risers reducing the efficiency of the base material but preventing its failure by planes perpendicular to the stress.
5 The usage of Timberfill should be limited to workpieces where aspect is more important than function.

Conflicts of interest

On behalf of all authors, the corresponding author states that the authors declare that they have no known competing financial interests or personal relationships that could have appeared to influence the work reported in this paper.

Acknowledgements

The authors want to thank Filamentum Ltd. for providing them with the materials necessary to the undertaking of the experiments.

REFERENCES

[1] Jerez-Mesa R, Travieso-Rodriguez JA, Corbella X, Busqué R, Gomez-Gras G. Finite element analysis of the thermal behavior of a RepRap 3D printer liquefier. Mechatronics 2016;36:119–26.
[2] Jerez-Mesa R, Gomez-Gras G, Travieso-Rodriguez JA, Garcia-Plana V. A comparative study of the thermal behavior of three different 3D printer liquefiers. Mechatronics 2018;56:297–305.
[3] Gomez-Gras G, Jerez-Mesa R, Travieso-Rodriguez JA, Lluma-Fuentes J. Fatigue performance of fused filament fabrication PLA specimens. Mater Des 2018;140:278–85.
[4] Pringle AM, Rudnicki M, Pearce JM. Wood furniture waste–Based recycled 3-D printing filament. For Prod J 2018;68(1):86–95.
[5] Zhao DX, Cai X, Shou GZ, Gu YQ, Wang PX. Study on the preparation of bamboo plastic composite intend for additive manufacturing. Key Eng Mater 2015;667:250–8.
[6] Ochi S. Mechanical properties of kenaf fibers and kenaf/PLA composites. Mech Mater 2008;40:446–52.
[7] Oksman K, Skrifvars M, Selin JF. Natural fibres as reinforcement in polylactic acid (PLA) composites. Compos Sci Technol 2002;3:1317–24.
[8] Huber T, Müssig J. Fibre matrix adhesion of natural fibres cotton, flax and hemp in polymeric matrices analyzed with the single fiber fragmentation test. Compos Interfaces 2008;15:335–49.
[9] Tao Y, Wang H, Li Z, Li P, Shi SQ. Development and application of wood flour-filled polylactic acid composite filament for 3D printing. Materials 2017;10:339.
[10] Kariz M, Sernek M, Obućina M, Kuzman MK. Effect of wood content in FDM filament on properties of 3D printed parts. Mater Today Commun 2017;14:135–40.
[11] Lin W, Xie G, Qiu Z. Effects of aging on properties of wood flour–Poly (Lactic acid) 3D printing filaments. BioResources 2019;14(4):8689–700, 18.
[12] Ozdemir F, Ayrilmis N, Kaymakci A, Kwon JH. Improving dimensional stability of injection molded wood plastic composites using cold and hot water extraction methods. Maderas Cienc Y Tecnol 2014;16(3):365–72.
[13] Daver F, Lee KP, Brandt M, Shanks R. Cork–PLA composite filaments for fused deposition modelling. Compos Sci Technol 2018;168:230–7.
[14] Gkartzou E, Koumoulos EP, Charitidis CA. Production and 3D printing processing of bio-based thermoplastic filament. Manuf. Rev 2017;4:1.
[15] Depuydt D, Balthazar M, Hendrickx K, Six W, Ferraris E, Desplentere F, et al. Production and characterization of

bamboo and flax Fiber reinforced polylactic acid filaments for fused deposition modeling (FDM). Polym Compos 2019;40:1951–63.
[16] Tisserat B, Joshee N, Mahapatra AK, Selling GW, Finkenstadt VL. Physical and mechanical properties of extruded poly (lactic acid)-based Paulownia elongata biocomposites. Ind Crops Prod 2013;44:88–96.
[17] Guo R, Ren Z, Bi H, Song Y, Xu M. Effect of toughening agents on the properties of poplar wood Flour/Poly (lactic acid) composites fabricated with fused deposition modeling. Eur Polym J 2018;107:34–45.
[18] Filgueira D, Holmen S, Melbø JK, Moldes D, Echtermeyer AT, Chinga-Carrasco G. Enzymatic-assisted modification of thermomechanical pulp fibers to improve the interfacial adhesion with poly (lactic acid) for 3D printing. ACS Sustain Chem Eng 2017;5:9338–46.
[19] Ayrilmis N, Kaymakci A, Ozdemir F. Physical, mechanical, and thermal properties of polypropylene composites filled with walnut shell flour. Ind Eng Chem 2013;19(3):908–14.
[20] Yang TC. Effect of extrusion temperature on the physico-mechanical properties of unidirectional wood fiber-reinforced polylactic acid composite (WFRPC) components using fused deposition modeling. Polymers 2018;10(9):976.
[21] Xie G, Zhang Y, Lin W. Plasticizer combinations and performance of wood flour–Poly (Lactic acid) 3D printing filaments. BioResources 2017;12:6736–48.
[22] Stoof D, Pickering K, Zhang Y. Fused deposition modelling of natural Fibre/Polylactic acid composites. J Compos Sci 2017;1:8.
[23] Ayrilmis N, Dundar T, Kaymakci A, Ozdemir F, Kwon JH. Mechanical and thermal properties of wood-plastic composites reinforced with hexagonal boron nitride. Polym Compos 2014;35(1):194–200.
[24] Sood AK, Ohdar RK, Mahapatra SS. Parametric appraisal of mechanical property of fused deposition modelling processed parts. Mater Des 2010;31(1):287–95.
[25] Domingo-Espin M, Puigoriol-Forcada JM, Garcia-Granada AA, Llumà J, Borros S, Reyes G. Mechanical property characterization and simulation of fused deposition modeling polycarbonate parts. Mater Des 2015;83:670–7.
[26] Domingo-Espin M, Travieso-Rodriguez JA, Jerez-Mesa R, Lluma-Fuentes J. Fatigue performance of ABS specimens obtained by fused filament fabrication. Materials 2018;11(12):2521–36.
[27] Tymrak BM, Kreiger M, Pearce JM. Mechanical properties of components fabricated with open-source 3-D printers under realistic environmental conditions. Mater Des 2014;58:242–6.
[28] Singh R. Some investigations for small-sized product fabrication with FDM for plastic components. Rapid Prototyp J 2013;19(1):58–63.
[29] Durgun I, Ertan R. Experimental investigation of FDM process for improvement of mechanical properties and production cost. Rapid Prototyp J 2014;20(3):228–35.
[30] Jerez-Mesa R, Travieso-Rodriguez JA, Lluma-Fuentes J, Puig D. Fatigue lifespan study of PLA parts obtained by additive manufacturing. Procedia Manuf 2017;13:872–9.
[31] Singh R. Process capability analysis of fused deposition modelling for plastic components. Rapid Prototyp J 2013;20(1):69–76.
[32] Wahl L, Maas S, Waldmann D, Zurbes A, Freres P. Shear stresses in honeycomb sandwich plates: analytical solution, finite element method and experimental verification. J Sandw Struct Mater 2012;14(4):449–68.
[33] Spierings AB. Fatigue performance of additive manufactured metallic parts. Rapid Prototyp J 2013;19(2):88–94.
[34] Edwards P, Ramulu M. Fatigue performance evaluation of selective laser melted Ti-6Al-4V. Mater Sci Eng A 2014;598:327–37.
[35] Riemer A, Leuders S, Thöne M, Richard HA, Tröster T, Niendorf T. On the fatigue crack growth behavior in 316L stainless steel manufactured by selective laser melting. Eng Fract Mech 2014;120:15–25.
[36] Afrose MF, Masood SH, Iovenitti P, Nikzad M, Sbarski I. Effects of part build orientations on fatigue behaviour of FDM-processed PLA material. Prog Addit Manuf 2016;1(1):21–8.
[37] Taguchi G, Chowdhury S, Wu Y. Taguchi's quality engineering handbook. Hoboken: John Wiley & Sons; 2005.
[38] ASTM. D7774-12 Standard Test method for flexural fatigue properties of plastics. West Conshohocken: ASTM International; 2013.
[39] Wirsching PH, Light MC. Fatigue under wide band random stresses. J Struct Div 1980;106(7):1593–607.
[40] Burhan I, Kim HS. S-N curve models for composite materials characterisation: an evaluative review. J Compos Sci 2018;2:38.